Long-range behavior and frequency dependence of exchange-correlation kernels in solids

Rodolfo Del Sole and Giovanni Adragna
Istituto Nazionale per la Fisica della Materia, Dipartimento di Fisica dell'Università di Roma Tor Vergata, Via della Ricerca Scientifica, I-00133 Roma, Italy

Valerio Olevano and Lucia Reining
Laboratoire des Solides Irradiés UMR 7642, CNRS-CEA/DSM, École Polytechnique, F-91128 Palaiseau, France
(Received 15 November 2002; published 31 January 2003)

We define an effective exchange-correlation kernel f_{xc}^{eff} which allows us to obtain correct absorption and energy loss spectra starting from an electronic structure obtained within some given approximation. We consider, in particular, the Kohn Sham electronic structure calculated in the local-density approximation and that obtained from a quasiparticle calculation. We show that in both cases the main feature able to account for the experimental spectra is a sizable, complex, and frequency- and material-dependent long-range contribution to f_{xc}^{eff}. We write, in terms of this contribution, an expression for the macroscopic dielectric function which is a generalization of the well-known contact-exciton approximation. Accurate absorption (for silicon and diamond) and electron energy loss (for silicon) spectra are obtained.

DOI: 10.1103/PhysRevB.67.045207 PACS number(s): 71.10.−w, 71.15.Qe, 71.35.−y, 78.20.Bh

The description of many electronic spectra, such as, e.g., optical absorption, requires the inclusion of many-body and in particular excitonic (electron-hole interaction) effects.[1] Only recently and for relatively simple systems have these effects been included in *ab initio* calculations in the framework of many-body theory by the technically cumbersome solution of the Bethe-Salpeter equation (BSE).[2,3]

A good candidate for a computationally simpler approach is (the in principle exact) time-dependent density functional theory (TDDFT),[4] where the many-body effects are taken into account in the frequency-dependent exchange-correlation (xc) potential v_{xc} and its density functional derivative, the xc kernel f_{xc}, accounting for xc effects in the linear response. However, for real systems neither v_{xc} nor f_{xc} are known. Approximations are often derived from model systems like the homogeneous electron gas, a prominent example being the local-density approximation (LDA) for v_{xc} (Ref. 5) and the adiabatic local-density approximation (ALDA) for f_{xc}, f_{xc}^{ALDA} (Ref. 6). Concerning the optical properties of solids, these approximations fail even qualitatively. They are not able to reproduce neither self-energy nor excitonic effects, which can lead to wrong transition energies and to a lack of important spectral features.

It has been shown[7–9] that a crucial ingredient of f_{xc} in infinite systems is a long-range (LR) $1/|r-r'|$ tail which is *absent* in the xc kernel of the homogeneous electron gas. It is due to both self-energy contributions[7,8] and to excitonic effects.[9] The two contributions were predicted with positive and negative signs, respectively. It is not clear to which extent the two terms cancel or which one is possibly predominating in which energy region. Some of us have shown[9] that an f_{xc} of the form $f_{xc}=-\alpha/|\mathbf{r}-\mathbf{r}'|$, where α is simply a material- and screening-dependent constant, describes well continuum exciton effects in the optical spectrum of simple semiconductors when self-energy corrections are already included in the independent-quasiparticle polarizability, but that a constant α is *not* sufficient to yield at the same time the loss spectra or bound excitons.[10]

In order to improve this situation, one can proceed in two directions. First, one can go beyond the simplest approximation used in Ref. 9 either by including a frequency dependence in α or a more complicated spatial variation in the xc kernel, or both. Second, one can make use of the freedom to change the starting point—i.e., the electronic structure which yields the independent-particle polarizability—and try to find out if a particular choice is the most suitable one in order to allow for a relatively simple associated kernel.

In this paper we address both questions. First, we define an *effective xc kernel* f_{xc}^{eff}, to be used in conjunction with a given starting electronic structure, by requiring that it must yield the correct macroscopic dielectric function. As starting points, we consider the cases of the DFT-LDA Kohn-Sham electronic structure and of a quasiparticle electronic structure as obtained in the GW approximation.[11] We write the LR component of f_{xc}^{eff} in terms of the starting independent-(quasi)particle polarizability and of the full result including self-energy corrections and the electron-hole (e-h) interaction.[2] We then calculate approximatively this LR component and show that it is non-negligible, complex, material dependent, and with a sizable frequency dependence that is displayed here for the first time in real materials.[21] We discuss which of these features are important and in which context. Finally, we derive an exact expression for the macroscopic dielectric function in a form that closely resembles the contact-exciton approximation,[12] showing that the effective contact e-h interaction is proportional to the LR component of f_{xc}. We apply this expression to the case of bulk silicon and diamond and demonstrate that the dynamical LR contribution alone is sufficient to obtain excellent agreement with Bethe-Salpeter calculations and with experiment in the case of both optical absorption and energy loss spectra.

The charge density induced by a time-dependent pertur-

bation is described by the irreducible polarizability $P(\mathbf{r},\mathbf{r}';t-t')$. Within TDDFT, its time Fourier transform $P(\mathbf{r},\mathbf{r}';\omega)$ is given by

$$P(\mathbf{r},\mathbf{r}';\omega)=\chi^{(0)}(\mathbf{r},\mathbf{r}';\omega)+\int d^3\mathbf{r}_1\, d^3\mathbf{r}_2\, \chi^{(0)}(\mathbf{r},\mathbf{r}_1;\omega) \times f_{xc}(\mathbf{r}_1,\mathbf{r}_2;\omega)P(\mathbf{r}_2,\mathbf{r}';\omega), \quad (1)$$

where $\chi^{(0)}$ is the independent-particle response function and f_{xc} is the xc kernel. Here $\chi^{(0)}$ is assumed to be the exact Kohn-Sham polarizability, based on the band structure calculated using the *exact* xc potential v_{xc}. The latter being unknown, some approximation to it must be used. As a consequence, the f_{xc} yielding the exact P in Eq. (1) is then not the true xc kernel, defined as the density functional derivative of the exact xc potential. Nevertheless, Eq. (1) can be used to define a suitable f_{xc}^{eff}: for any approximate $\chi_{\mathrm{appr}}^{(0)}$, there is an f_{xc}^{eff} which allows Eq. (1) to yield the exact polarizability P,

$$P=\chi_{\mathrm{appr}}^{(0)}+\chi_{\mathrm{appr}}^{(0)}f_{xc}^{\mathrm{eff}}P. \quad (2)$$

The exact f_{xc}—i.e., the functional derivative of the xc potential—is recovered only when $\chi_{\mathrm{appr}}^{(0)}$ coincides with the exact Kohn-Sham polarizability. Hence, if we use Kohn-Sham DFT-LDA eigenvalues to calculate an approximate $\chi_{\mathrm{LDA}}^{(0)}$, we have to introduce an effective f_{xc}^{FLDA} (the superscript means "from LDA"; this kernel should not be confused with f_{xc}^{ALDA}) to obtain the exact polarizability P from Eq. (2). Analogously, if we start from an independent-quasiparticle polarizability $\chi_{\mathrm{QP}}^{(0)}=-iGG$ and calculate the Green's function G using quasiparticle (for example, GW) energies, we can define another effective xc kernel f_{xc}^{FQP} (a many-body analog of f_{xc}) through

$$P=\chi_{\mathrm{QP}}^{(0)}+\chi_{\mathrm{QP}}^{(0)}f_{xc}^{\mathrm{FQP}}P. \quad (3)$$

In fact the approach of Ref. 9, based on the GW band structure, deals with f_{xc}^{FQP}.

Equation (2) can be solved for f_{xc}^{eff}, giving

$$f_{xc}^{\mathrm{eff}}=\chi_{\mathrm{appr}}^{(0)^{-1}}-P^{-1}, \quad (4)$$

which is analogous to a well-known equation[13] that holds for the exact f_{xc}.

Using the relation $\varepsilon=1-vP$ (v is the coulombian potential) and Eq. (4), we obtain f_{xc} in terms of the full dielectric function ε and of $\varepsilon_{\mathrm{appr}}^{\mathrm{RPA}}=1-v\chi_{\mathrm{appr}}^{(0)}$:

$$f_{xc}^{\mathrm{eff}}=[(\varepsilon-1)^{-1}-(\varepsilon_{\mathrm{appr}}^{\mathrm{RPA}}-1)^{-1}]v. \quad (5)$$

From Eq. (5) one can in principle calculate the effective kernel. One has to determine $\varepsilon_{\mathrm{appr}}^{\mathrm{RPA}}$ and to know a very good approximation for ε—for example, the result of a Bethe-Salpeter calculation. However, since Eq. (5) is a matrix equation involving microscopic quantities, one would need much more information from the Bethe-Salpeter equation than the sole macroscopic spectra that are usually calculated. Rather, we concentrate here on the LR component of f_{xc}^{eff} in a solid, namely the head of its spatial Fourier transform $f_{xc}^{\mathrm{eff}}(\mathbf{q},\omega)_{00}$, where the subscript 00 stands for vanishing reciprocal lattice vectors $\mathbf{G}=\mathbf{G}'=0$ and where the vector $\mathbf{q}$ in the first Brillouin zone tends to zero. As we will show in the following, this allows us to describe all the essential physics using only quantities which have already been calculated in the past.

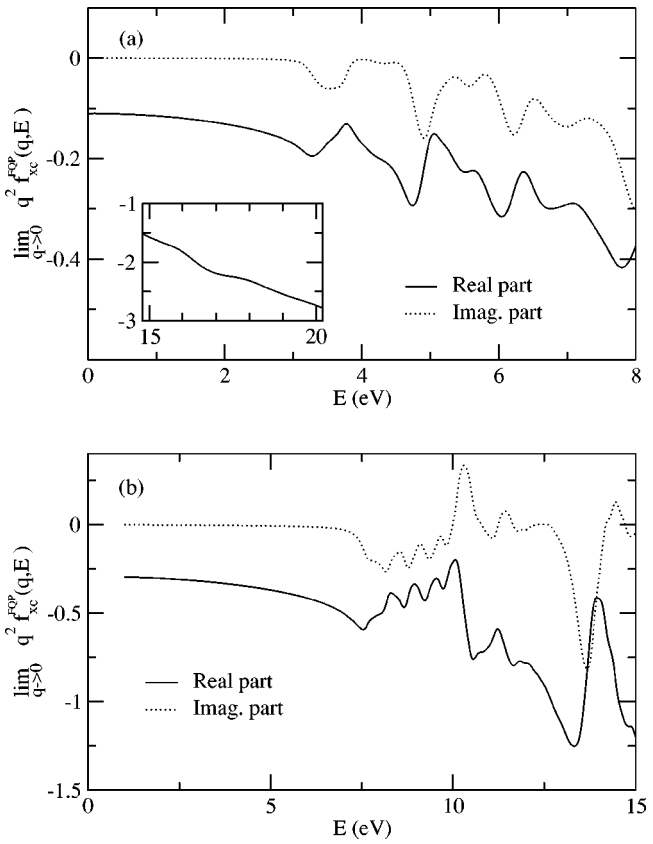

FIG. 1. Long-range component of the many-body exchange-correlation kernel f_{xc}^{FQP}. (a) Si and (b) diamond. The inset in (a) shows the real part of the LR kernel of Si close to the plasma frequency.

Keeping in mind that in the range of an optical spectrum of a semiconductor the screening is much larger than 1, we neglect 1 with respect to ε and $\varepsilon_{\mathrm{appr}}^{\mathrm{RPA}}$ in Eq. (5). This yields

$$f_{xc}^{\mathrm{eff}}(\mathbf{q},\omega)_{00}=[\varepsilon(\mathbf{q},\omega)_{00}^{-1}-\varepsilon_{\mathrm{appr}}^{\mathrm{RPA}}(\mathbf{q},\omega)_{00}^{-1}]v_0(q). \quad (6)$$

Both inverse macroscopic dielectric functions correctly account for local field effects. The neglected terms, estimated without local field effects, result in being hardly visible in the scale of our figures.

Calculations of the dielectric functions have been carried out for silicon and diamond as in Ref. 2. Figure 1 shows $q^2 f_{xc}^{\mathrm{FQP}}(\mathbf{q},\omega)$ for $\mathbf{q}\to 0$. Since this quantity accounts for the e-h interaction alone, while the f_{xc}^{FLDA} kernel accounts also for self-energy effects, it has a simpler physical meaning. Its real part is negative in the optical range, describing an attractive e-h interaction. It is, however, far from being constant as a function of ω, since it changes by a factor of 3 going through the range of strong optical absorption. Here its average value is about -0.2 in Si and -0.6 for diamond, consistent with the suggestion of Refs. 9 and 10. The imaginary

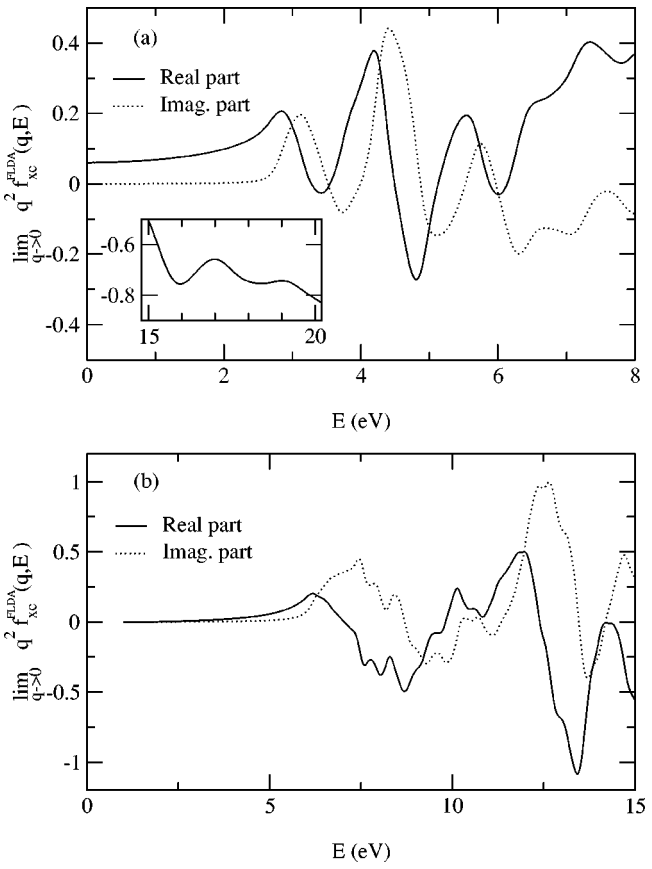

FIG. 2. Long-range component of the effective xc kernel f_{xc}^{FLDA}. (a) Si and (b) diamond. The inset in (a) shows the real part of the LR kernel of Si close to the plasma frequency.

part is nonzero above the direct gap and smaller than the real part, with oscillations leading also to positive values for diamond.

Figure 2 shows $q^2 f_{xc}^{\mathrm{FLDA}}(\mathbf{q},\omega)$; it is generally smaller than $q^2 f_{xc}^{\mathrm{FQP}}$, because of the partial cancellation of self-energy and *e-h* interaction effects, while its ω dependence is stronger. Differently from the case of f_{xc}^{FQP}, the imaginary and real parts are comparable. Accounting for two effects, its interpretation is less straightforward. Different results are obtained for Si and diamond for both kernels, those related to diamond being greater in absolute value. In spite of this, $q^2 f_{xc}^{\mathrm{FLDA}}$ of diamond vanishes for zero frequency, as a consequence of a complete cancellation of self-energy and *e-h* interaction effects, which leads to equal BSE and LDA random phase approximation (RPA) static dielectric constants. The rich frequency dependence of the kernels considered here is related, through Eq. (6), to the variation (due to *e-h* interaction and self-energy effects) of the longitudinal *e-h* excitations entering the inverse dielectric functions. Being differences of causal inverse polarizabilities, they obey the Kramers-Kronig relation.[14] This is also clearly visible in Figs. 1 and 2, where the imaginary parts look like plus or minus an absorptive response function, while the real parts are similar to the dispersive counterparts.

Since it has been shown in Ref. 10 that an average static α can yield good absorption spectra for the materials considered here, but the same α *cannot* describe the plasmon, it is particularly interesting to extend the range of frequencies to higher energies. However, the plasmon arises at frequencies where the macroscopic dielectric function is close to zero, and we have to make a different expansion than above: we assume that all the relevant dielectric functions are smaller than unity. This is true between 16 and 18 eV in Si.[15] Hence we expand Eq. (5) to first order in the dielectric functions, which yields results similar to Eq. (6), but with the dielectric functions instead of their inverse. The results for the two kernels in Si are shown in the insets of Figs. 1(a) and 2(a). Their real parts are both shifted towards lower values, which makes now both f_{xc}^{eff} become completely negative, in contrast to the optical range. The imaginary parts of $q^2 f_{xc}^{\mathrm{FLDA}}$ and $q^2 f_{xc}^{\mathrm{FQP}}$ are both positive, of the order of 0.5.

Interestingly, the LR component of the two kernels is sufficient in order to obtain very good spectra: if we consider the matrix f_{xc}^{eff} to be only $f_{xc}^{\mathrm{eff}}(\mathbf{q},\omega)_{\mathbf{GG}'}=4\pi g(\omega)/q^2$ if $\mathbf{G}=\mathbf{G}'=0$, and $f_{xc}^{\mathrm{eff}}(\mathbf{q},\omega)_{\mathbf{GG}'}=0$ otherwise, the equations

$$\varepsilon_{\mathrm{M}}=1-\frac{4\pi}{q^2}\overline{P}_{00}, \tag{7}$$

$$\overline{P}=\chi_{\mathrm{appr}}^{(0)}+\chi_{\mathrm{appr}}^{(0)}(\overline{v}+f_{xc}^{\mathrm{eff}})\overline{P}, \tag{8}$$

where $\overline{v}$ is the Coulomb potential with its $\mathbf{G}=0$ element set to zero,[16] yield

$$\varepsilon_{\mathrm{M}}(\omega)=1+\frac{\varepsilon_{\mathrm{M}}^{\mathrm{appr}}(\omega)-1}{1+g(\omega)[\varepsilon_{\mathrm{M}}^{\mathrm{appr}}(\omega)-1]}, \tag{9}$$

where $g(\omega)=\lim_{\mathbf{q}\to 0} q^2 f_{xc}^{\mathrm{eff}}(\mathbf{q},\omega)/4\pi$ and $\varepsilon_{\mathrm{M}}^{\mathrm{appr}}(\omega)$ is the macroscopic dielectric function relative to the approximation scheme used in Eq. (4). Note that through $\overline{v}$ we have fully included local-field effects everywhere.[17] One can see the close resemblance of Eq. (9) with the old contact-exciton approximation.[12] There, the contact electron-hole interaction was described by a real constant, while here it is given by a complex and frequency-dependent quantity $g(\omega)$. The contact-exciton parameter is hence directly related to the coefficient of the LR divergence of the xc kernel.

The dielectric function of bulk silicon calculated according to Eq. (9) is plotted in Fig. 3. The small difference to the result obtained solving the Bethe-Salpeter equation is due to the approximations made in deriving the LR components of the kernels and to the neglect of the microscopic components. The similarity of these calculations to the BSE result confirms that both approximations are very good. Similar good results, not shown here, are obtained for diamond. This implies that the kernels displayed in the figures are perfectly representative for the quantities one is searching for, and it is most instructive to discuss the effects of their features on the resulting spectra. It turns out that starting from a quasiparticle electronic structure allows one to use a simpler approximation to f_{xc}^{eff} than starting from LDA: in the former case, indeed, a good spectrum is obtained by neglecting the imaginary part of f_{xc}^{FQP} and by approximating the real part as a

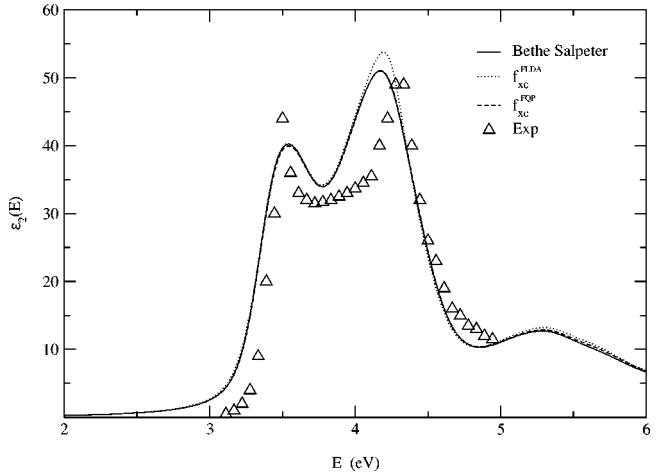

FIG. 3. Imaginary part of the macroscopic dielectric function of Si. Solid line: including the electron-hole interaction by solving the Bethe-Salpeter equation, as in Ref. 2; Dashed line: calculated according to Eq. (9) using $\chi_{\mathrm{QP}}^{(0)}$ and f_{xc}^{FQP}. Dotted line: calculated according to Eq. (9) but using $\chi_{\mathrm{LDA}}^{(0)}$ and f_{xc}^{FLDA}. Triangles: experiment (Ref. 19).

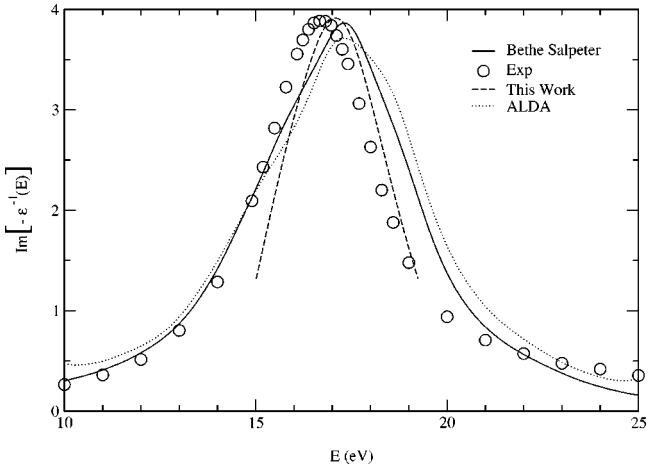

FIG. 4. Loss function of Si: Circles: experiment (Ref. 20). Solid line: BSE result (Ref. 15). Dotted line: ALDA result. Dashed line: result of Eq. (9) using f_{xc}^{FLDA}. The calculated curves embody a Lorentzian broadening of 0.75 eV.

suitable constant, as has been done in Ref. 9. Neither of the two approximations leads to satisfactory spectra when starting from the LDA. In this context it is also interesting to note that a recently published so-called ''EXX TDDFT'' calculation[18] finds good results for the absorption spectrum of silicon using again a static, long-range kernel (with a prefactor containing an empirical correction): the starting KS band structure in that case is in fact close to the GW one.

The TDDFT energy loss spectrum of Si, calculated according to Eq. (9), is shown in Fig. 4. When starting from GW, the contribution of the long-range part is important, since the GW spectrum is strongly shifted towards higher energies, and the effect of the kernel f_{xc}^{FQP} is to compensate this shift and bring the plasmon back to the right position. Since the ALDA spectrum (dotted line) is already rather good,[15] the improvement due to the kernel f_{xc}^{FLDA} is not drastic, but it is, however, significant. In particular, slightly worse results are obtained if the imaginary part of the xc kernel is neglected.

In conclusion, we have derived expressions for effective xc kernels f_{xc}^{eff}, in particular for the case that one starts with an LDA electronic structure, f_{xc}^{FLDA}, and for the case of a quasiparticle calculation, f_{xc}^{FQP}. Both kernels are complex and have a sizable long-range component with an important ω dependence. We have established a link to the old contact-exciton approach with an effective, complex, and frequency-dependent, on-site electron-hole interaction. This relation allows for a quick calculation of the spectra starting from the independent-(quasi)particle ones. Calculations carried out for bulk silicon and diamond yield very good agreement with experimental absorption and energy loss results. This work has allowed us to point out which are the important parameters of the respective kernels and their effect on the spectra. Therefore, it opens the way for a well directed search of effective exchange-correlation kernels and efficient calculations of electronic spectra.

This work has been supported in part by the INFM PRA 1MESS and by the EU through the NANOPHASE Research Training Network (Contract No. HPRN-CT-2000-00167). Computer time has been granted by IDRIS Project No. 544. The calculations have been done using the codes LSI-CP for ground state, DP for TDDFT, LSI-G*W* for G*W* and EXC for Bethe-Salpeter calculations (http://129.104.22.18/codes/codes.html).

[1] See, e.g., W. Hanke and L.J. Sham, Phys. Rev. Lett. **43**, 387 (1979); Phys. Rev. B **21**, 4656 (1980).
[2] G. Onida, L. Reining, R.W. Godby, R. Del Sole, and W. Andreoni, Phys. Rev. Lett. **75**, 818 (1995); S. Albrecht, L. Reining, R. Del Sole, and G. Onida, *ibid.* **80**, 4510 (1998).
[3] L.X. Benedict, E.L. Shirley, and R.B. Bohn, Phys. Rev. B **57**, R9385 (1998); M. Rohlfing and S.G. Louie, Phys. Rev. Lett. **81**, 2312 (1998): B. Arnaud and M. Alouani, Phys. Rev. B **63**, 085208 (2001).
[4] E. Runge and E.K.U. Gross, Phys. Rev. Lett. **52**, 997 (1984); E.K.U. Gross and W. Kohn, *ibid.* **55**, 2850 (1985).
[5] W. Kohn and L.J. Sham, Phys. Rev. **140**, A1133 (1965).
[6] A. Zangwill and P. Soven, Phys. Rev. A **21**, 1561 (1980); for a recent application, see I. Vasiliev, S. Öğüt, and J.R. Chelikowsky, Phys. Rev. Lett. **82**, 1919 (1999).
[7] Ph. Ghosez, X. Gonze, and R.W. Godby, Phys. Rev. B **56**, 12 811 (1997); X. Gonze, Ph. Ghosez, and R.W. Godby, Phys. Rev. Lett. **74**, 4035 (1995).
[8] W.G. Aulbur, L. Jonsson, and J.W. Wilkins, Phys. Rev. B **54**, 8540 (1996).

[9] L. Reining, V. Olevano, A. Rubio, and G. Onida, Phys. Rev. Lett. **88**, 066404 (2002).
[10] S. Botti, F. Sottile, N. Vast, V. Olevano, L. Reining, A. Rubio, and G. Onida (unpublished).
[11] L. Hedin and S. Lundquist, in *Solid State Physics*, edited by H. Herenreich, F. Seitz, and D. Turnbull (Academic, New York, 1969), Vol. 23, p. 1.
[12] J.E. Rowe and D.E. Aspnes, Phys. Rev. Lett. **25**, 162 (1970); R.M. Martin, J.A. Van Vechten, J.E. Rowe, and D.E. Aspnes, Phys. Rev. B **6**, 2500 (1972).
[13] P. Streitenberger, Phys. Status Solidi B **125**, 681 (1984).
[14] R. Nifosi, S. Conti, and M.P. Tosi, Phys. Rev. B **58**, 12 758 (1998).
[15] V. Olevano and L. Reining, Phys. Rev. Lett. **86**, 5962 (2001).
[16] G. Onida, L. Reining, and A. Rubio, Rev. Mod. Phys. **74**, 601 (2002), Appendix A.
[17] It can be shown that Eq. (9) is valid also if $\varepsilon_{\mathrm{M}}^{\mathrm{appr}}$ includes the microscopic components of f_{xc}^{eff}—namely, those with **G** and/or $\mathbf{G}'$ different from zero.
[18] Y.H. Kim and A. Görling, Phys. Rev. Lett. **89**, 096402 (2002).
[19] P. Lautenschlager, M. Garriga, L. Vina, and M. Cardona, Phys. Rev. B **36**, 4821 (1987).
[20] J. Stiebling, Z. Phys. B **31**, 355 (1978).
[21] This is hence an alternative to the work in Ref. 9, where Eq. (9) suggests a spatially complex, but always static, f_{xc}.